Investigation of the Processes of Electron Injection during Dissolution of p-Si in Acidic Fluoride and Alkaline Media

Sandro Cattarin*

Istituto di Polarografia ed Elettrochimica Preparativa del C.N.R., Corso Stati Uniti 4, 35100 Padova, Italy

Laurence M. Peter and D. Jason Riley

School of Chemistry, University of Bath, Bath BA2 7AY, United Kingdom

Received: November 25, 1996; In Final Form: March 9, 1997[⊗]

The phenomena of electron injection occurring during anodic dissolution of Si are studied in a dual-electrolyte transistor-like geometry: variations in the population of minority carriers of a p-Si wafer resulting from injection are detected by a second liquid junction on the back side of the electrode. Investigations in acidic fluoride media show that electrons injected during porous silicon formation undergo ready surface recombination. A significant back current is detected in the electropolishing regime, indicating that important injection processes occur even under the latter conditions. Analogous investigations at p-Si in 2 M KOH show electron injection in correspondence to the oxidation peak leading to passivation. Results are compared with literature data and discussed with reference to current models of silicon dissolution.

1. Introduction

The processes of anodic (photo)dissolution of Si in acidic fluoride media have been extensively investigated over the last 4 decades. After the pioneering work devoted to etching and electropolishing,[1−2] a number of publications have appeared focused either on treatments of technological interest or on fundamental aspects of the electrochemical phenomena.

The current−potential curves recorded at p-Si in the dark (or at n-Si under illumination) show a typical form:[3−5] on sweeping the electrode potential from open circuit in a positive direction, the curves show a sharp rise of the anodic current after onset, a first narrow peak followed by a small plateau, a second broad peak and a subsequent large plateau in which, depending on experimental conditions, damped or sustained current oscillations may arise.[4−7] *In situ* and *ex situ* spectroscopic investigations have shown modifications of the electrode surface in the different potential regions. The hydrogen termination present at the open circuit and during porous silicon formation[8] is replaced by a "wet" oxide (hydroxide) layer over the potential region extending to the second broad peak,[9−10] then by a "dry" oxide similar to that obtained by thermal oxidation going further positive into the electropolishing plateau.[9−10] The average dissolution valence increases gradually from two electrons per dissolved silicon atom in the region of porous silicon formation to almost four in the electropolishing regime (see e.g. ref 11 and references therein). Divalent silicon dissolution is accompanied by H_2 evolution,[12] resulting from chemical reduction of protons by Si(II) species which are thereby oxidized to Si(IV). At n-Si, photocurrent quantum yields close to 4 are observed at very low light intensities,[5,13−15] indicating injection of three electrons for each photogenerated hole. On increasing the light intensity, the quantum yield decreases gradually to 2, with a concomitant increase of H_2 evolution from zero to one H_2 molecule for each dissolved Si(IV) atom.

A specific contribution to understanding the phenomena of electron injection during silicon dissolution may be expected from investigations at p-Si electrodes in a transistor-like geometry (refs 16−18 and references therein). In these experiments the working electrode, like the base of a transistor, is part of two circuits. On one side the electrode is in contact with the electrolyte selected for study and is polarized to induce dissolution. A junction is made at the back interface with another semiconductor (p−n junction, see ref 16) or an electrolyte[17] and polarized under reverse bias in the region of limiting current by a second circuit. If the dissolution processes at the front interface entail injection of electrons, and the latter have diffusion lengths comparable with the sample thickness, then variations in the population will extend through the sample bulk and will be detected as variations of the back limiting current.

Similar experiments had been performed by Memming and Schwandt,[19] who made use of a p−n junction for the back collection of minority carriers. Investigations were only reported for a limited potential range around open circuit. In the region of porous silicon formation, negligible current was observed in the back indicator circuit, and the authors concluded that divalent dissolution of p-Si in fluoride medium proceeds by capture of two holes from the valence band. This conclusion contrasts with the observation of a quantum yield of 2 during (photo)-electrodissolution of n-Si, which implies the mechanism now generally accepted that divalent oxidation results by a first act of hole capture followed by electron injection.[5]

To better elucidate the phenomena, we present an investigation performed over an extended potential range, from hydrogen evolution to electropolishing, carried out in a dual electrolyte arrangement similar to that used by Pleskov for investigations at a thin slice of n-Ge.[17] In order to get a more general picture, results are compared with those obtained during anodic dissolution of p-Si in 2 M KOH. Some aspects of the dissolution in alkaline media strongly suggest the presence of electron injection mechanisms: a similar dissolution peak, in about the same potential range, is observed during voltammograms at both n- and p-Si, although the hole concentration necessary to sustain the anodic process is missing at n-Si.[20−23] Experiments

[⊗] Abstract published in *Advance ACS Abstracts,* April 15, 1997.

S1089-5647(96)03921-1 CCC: $14.00

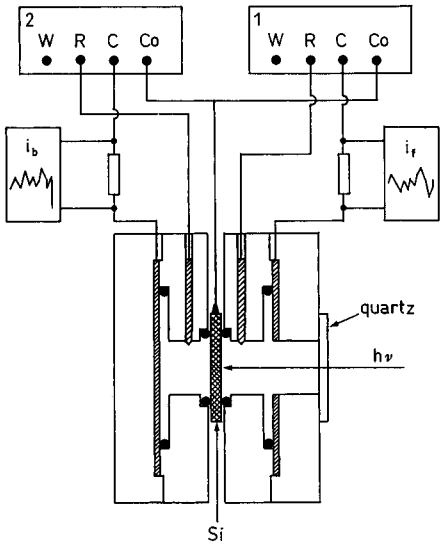

Figure 1. Scheme of the cell connections used to perform experiments in the transistor-like arrangement. The front circuit is used to polarize the electrode in the electrolyte of interest (either NH_4F or KOH). When necessary the interface is illuminated. The indicator circuit maintains the back interface (in contact with 1 M NH_4F, pH 4.5, which avoids oxide growth) polarized at $U = -2.0$ V vs Pt, in the region of a limiting cathodic current. Method of current measurement described in the Experimental Section.

proposed in the following discussion may help in better characterizing the phenomena.

2. Experimental Section

Bipolished p-Si wafers with (100) surface orientation, thickness of about 525 μm, and resistivity in the range 8−12 Ω cm were purchased from Wacker Chemie. Prior to electrochemical experiments the electrodes were etched for 60 s in a 1:1 mixture of 40% HF:ethanol to remove the oxide layer, rinsed with distilled water, and blown dry in a nitrogen stream. Solutions were prepared from analytical grade commercial products (BDH, Aldrich or Merck) and triply distilled water. Solutions of 1 M NH_4F were obtained by dilution of the semiconductor grade concentrated (12 M) solution (BDH) and adjusting the pH to about 4.5 with H_2SO_4 and NH_3.

Some experiments were performed in a cell in the traditional three-electrode arrangement, using an SCE reference (to which potentials are referred) and a platinum counter electrode. The samples, contacted with gallium−indium eutectic alloy, were mounted on mild steel strips and sealed with a PTFE coated adhesive tape (Cole Parmer Instruments). A circular hole in the sealing tape exposed to the solution a surface of 0.10−0.38 cm^2. Most experiments were carried out in the cell schematically reported in Figure 1, made from "Plexiglass" sheets. Platinum foils were inserted in the front compartment and in the back (dark) compartment. A hole in the front foil allowed electrode illumination. In order to simplify the experimental work involving use of HF, two Pt wires were used as (pseudo)-reference electrodes R_1 and R_2 in the two electrolyte compartments. The potential of the Pt electrode in 1 M NH_4F was $U \cong 0.15 \pm 0.10$ V vs SCE. The potential of the Pt electrode in 2 M KOH was $U \cong -0.15 \pm 0.05$ V vs SCE.

The electrochemical apparatus included potentiostats (Hi-Tek Instruments, England), which offer a connection to the (floating) common of the circuitry, and a function generator (Hi-Tek PPRI). The arrangement used for experiments in the dual electrolyte geometry is illustrated in Figure 1. The cell, similar

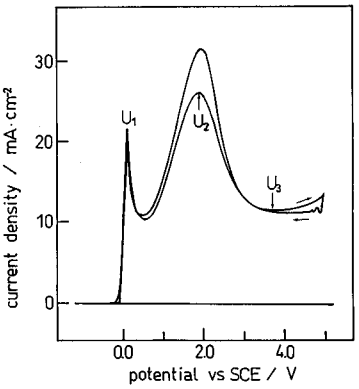

Figure 2. Cyclic voltammogram recorded with a p-Si electrode in 1 M NH_4F (scan rate 100 mV s^{-1}). The potentials U_1-U_3 divide the curve in four regions (see text).

to one described in detail elsewhere,[24] clamps a Si wafer acting as the working electrode between two separated electrolytic compartments, each provided with a Pt sheet counter electrode (CE) and a Pt wire (pseudo)reference electrode (R). An ohmic contact is made to the Si wafer, sealed on the front side by the PTFE adhesive tape with a circular hole exposing to the solution a surface of 0.10−0.38 cm^2. Electrochemical polarization is applied as shown in Figure 1, connecting the Si working electrode to the two common points of the potentiostats. The back (dark) interface is polarized under reverse bias at the constant potential $U = -2.0$ V vs Pt and the potential of the front (illuminated) interface is scanned. The current flowing in each circuit is measured as the voltage drop over a resistance in series to the counter electrode, and the signal is detected by a PM8278 Philips dual pen XY recorder with floating inputs. This type of measurement is preferred to that based on the current followers since connection in parallel of two operational amplifiers may result in unreliable measurements in both circuits.

Light sources were laser or ordinary light emitting diodes (LED) with wavelengths in the range 440−670 nm. Photon fluxes were measured with a calibrated silicon photodiode (SD112UV, Macam Photometrics). Reported photon fluxes are corrected for reflection losses. Photoelectrochemical experiments were performed with a conventional setup.[25,26]

3. Results

3.1. p-Si Dissolution in 1 M NH_4F. The open circuit potential is $U_{OC} \cong -0.46/-0.44$ V vs SCE. The flatband potential may be estimated as $U_{FB} \cong +0.10$ V vs SCE on the basis of the value for n-Si ($U_{FB} \cong -0.60$ V vs SCE),[27] although the real value may be somewhat more positive (e.g., $U_{FB} \cong +0.16$ V vs SCE estimated for p-Si in 0.1% HF, see ref 28). The current−voltage curve recorded in Figure 2 shows the well-known form characterized by two current maxima at about 0.1 V and 2.0 V vs SCE and a wide electropolishing plateau beyond the second peak. The curve, recorded at an electrode with small bulk resistance due to optimal geometry, shows little *iR* drop distortion and no oscillation in the current plateau region. Only a transient instability is triggered by the inversion of the potential scan direction at the positive limit, similar to literature reports.[7] Sustained current oscillations (not shown) arise at an applied voltage $U = 5$ V vs SCE if a resistance of 1 kΩ is inserted in series to a working electrode with a surface of about 0.10 cm^2. In analogy to a previous proposal,[5] we may identify in the current−potential curve three potential values which define four regions, to which different dissolution regimes/surface conditions may be associated:[5,9,10]

region I	$U < U_1$	porous silicon formation/ hydrogen terminated surface
region II	$U_1 < U < U_2$	electropolishing/surface covered by a "wet" oxide
region III	$U_2 < U < U_3$	electropolishing/surface covered by a "dry" oxide
region IV	$U_3 < U$	current oscillations/ periodic changes in oxide coverage

The division is obviously qualitative and transition from one to another regime is gradual.

3.1.1. Transistor-like Experiments in the Dark. As already indicated, in these experiments the back interface is polarized under depletion at a constant potential ($U = -2.0$ V vs Pt), in the region at which a small limiting cathodic current flows. The front interface is polarized to induce dissolution and the curves in Figure 3 are obtained. The distortion of curve 3a as compared to Figure 2 and the onset of current oscillations at the positive potential limit depend on the large resistance (on the order of 500−600 Ω) of samples suitable to fit in the given cell, which required electric contact at least 2 cm away from the "active" electrode area (0.10 cm^2). However, the usual regions I−IV may be identified in the curve and separated by the conventional potentials U_1−U_3.

As shown by Figure 3, the current at the back interface (line b) varies while scanning the potential of the front interface from open circuit in a positive direction through the various regions of the current−potential curve (line a). Similar to observations by Memming and Schwandt, a very low current is detected by the indicator circuit in the region I of porous silicon formation ($U < U_1$). On sweeping the electrode potential positive to U_1, the current in the indicator circuit starts increasing and describes a curve with a maximum at potentials significantly less anodic than U_2 (Figure 3) and a marked decrease in the region of the second electropolishing plateau, where current oscillations occur in both circuits.

To look more closely at the latter phenomenon, polarization was performed in a solution of diluted NH_4F (0.1 M), to get a lower oscillation frequency and to appreciate the phase relation between oscillations in the two circuits. Figure 4b shows that the periodic maxima in back current, i.e. in the rate of electron injection, precede the maxima in dissolution current (Figure 4a). In an independent experiment the admittance of the interface (excitation frequency of 2−3 kHz) was measured during oscillations. The imaginary part of admittance, proportional to the interface capacitance, oscillates with the same frequency of the current, and it may be reasonably assumed that this reflects periodic variations in the oxide thickness, a lower capacitance being associated with a thicker oxide. The maxima in capacitance (minima in oxide thickness) occur at the foot of the dissolution current peak, close to the injection current maxima.[29] Hence, it may be concluded that the injection rate attains its maximum when the oxide layer thickness is close to its minimum periodic value.

3.1.2. Transistor-like Experiments under Illumination. The relative values of the back current as shown and discussed in the previous section are controlled by the rates of injection and surface recombination processes, since the bulk recombination is not affected by interface modifications. In order to obtain reliable information on the relative injection rates, it is necessary to know more about surface recombination processes. The polarization experiments were therefore repeated under chopped illumination with visible light ($\lambda = 650$ nm, photon flux $I_0 \cong 1.14 \times 10^{15}$ s^{-1} cm^{-2}), which generates minority carriers in a thin layer close to the surface ($1/\alpha \cong 3.3$ μm). Although these carriers are generated deeper in the material as compared with those injected by the dissolving species, some similarity in the surface recombination processes may be expected.

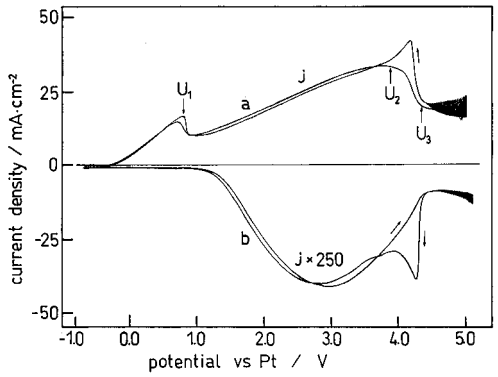

Figure 3. Experiment in a transistor-like arrangement. Electrolyte: 1 M NH_4F, pH ≅ 4.5 in both compartments. (upper curve a) Cyclic voltammogram at the front interface (scan rate 50 mV s^{-1}). Curve distorted by *iR* drop (R ≅ 500 Ω; electrode surface, 0.10 cm^{-2}); potentials U_1−U_3 (compare with Figure 2). (lower curve b) Current in the back indicator circuit, magnified 250 times; note small instrumental shift to the right (figure is a direct reproduction of curve obtained with the dual pen XY recorder).

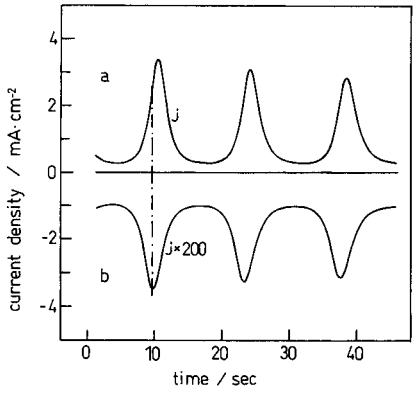

Figure 4. Experiment in a transistor-like arrangement. (upper curve a) Slow current oscillations at front interface ($U = 5$ V vs Pt, electrolyte: 0.86 M NH_4Cl, 0.10 M NH_4F, 0.04 ammonium acetate, 0.06 M acetic acid, pH adjusted to about 4.0). (lower curve b) Current in the indicator circuit, magnified 200 times. Vertical line shows phase relation.

Figure 5a shows the (photo)current−potential curve relevant to the front polarization circuit, corrected for *iR* drop. At the negative potential extreme, the front photocurrent $j_{f,ph}$ attains a limiting value $j_{f,ph} \cong I_0 e = j_0$, corresponding to unit quantum yield *Q*. On sweeping the potential in a positive direction, the photoeffect gradually disappears and the anodic curve of Si dissolution corresponds to that of Figure 2. Figure 5b shows the current recorded by the indicator circuit. The back photocurrent $j_{b,ph}$ (i.e. the difference between the currents recorded under illumination and in the dark) is negligible at the negative limit, since the photogenerated electrons are efficiently collected at the front contact. As the potential of the front interface increases, the back photocurrent increases, attains a maximum around the open circuit potential, and then drops, remaining small over the potential region I of porous silicon formation. Going further positive, it increases again reaching a second maximum at a potential between U_1 and U_2, then decreases to a low value in the second current plateau (Figure 5b). From the onset of dissolution to the positive potential limit, similar behavior is observed for the dark current (filled circles).

A comparison is better made on the basis of the ratio $R = j_b/j_f$ between the back-collected current j_b and the front-collected current j_f, whose values can be related to the "efficiency" of

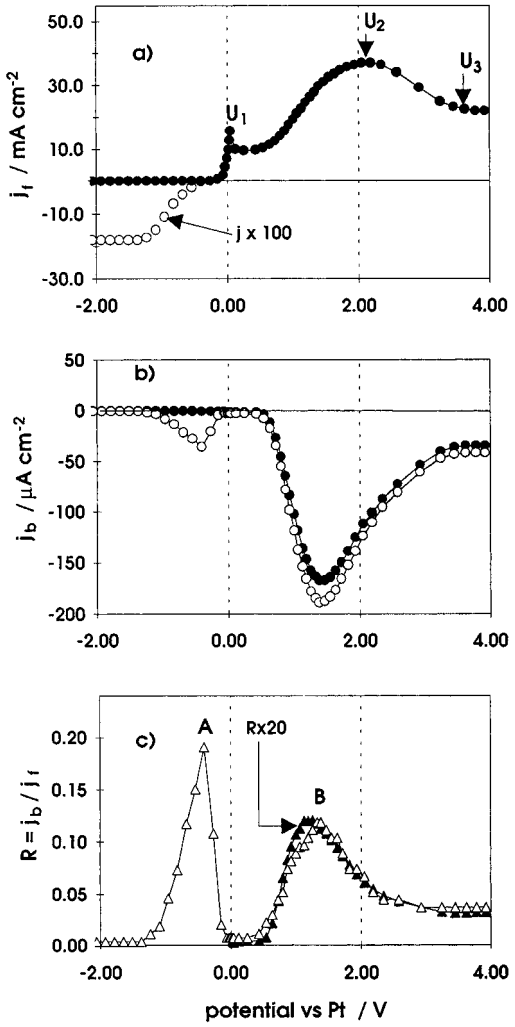

Figure 5. Experiments in a transistor-like arrangement. Electrolyte: 1 M NH_4F, pH ≅ 4.5 in both compartments. Figures show (a) dynamic current−potential curve (sweep from negative limit, scan rate 50 mV s^{-1}), recorded at the front interface in the dark (filled circles). Open circles represent the photocurrent (magnified 100 times) under a photon flux $I_0 \cong 1.14 \times 10^{15}$ s^{-1} cm^{-2}. Limiting photocurrent for unitary Q: $j_0 = I_0$ e ≅ 183 μA cm^{-2} (see plateau at negative limit); (b) corresponding curves recorded in the indicator circuit, when the front interface is in the dark (filled circles) and under illumination (open circles); and (c) comparison of the ratios $R = j_b/j_f$ for the conditions of dark (filled triangles, R values magnified 20 times) and light (open triangles). In the latter case the constant value $j_0 \cong 182$ μA cm^{-2} is used for j_f.

the collection experiments. The curve relevant to the photocurrent (Figure 5c, open triangles) is obtained from the ratios $R = j_{b,ph}/j_0$, in which $j_{b,ph}$ is the back photocurrent at the given potential and j_0 is the limiting photocurrent recorded at the front contact (see Figure 5a, negative potential limit). The curve in Figure 5c shows two maxima: the first (peak A) is observed with the front interface at the open circuit, the second (peak B) with the front interface polarized midway between U_1 and U_2, in the region of formation of a "wet" oxide on the electrode surface. The curve relevant to injection processes (filled triangles in Figure 5c) corresponds to ratios $R = j_b/j_f$ of currents in the dark. Only points corresponding to $j_f > 0$ (front dissolution) are reported in Figure 5c. The curve shows a maximum close to peak B of the photocurrent curve.

The photocurrent−potential curves relevant to light with wavelength $\lambda = 440$ nm ($1/\alpha \cong 200$ nm) show the same pattern observed in Figure 5 ($\lambda = 650$ nm, $1/\alpha \cong 3.3$ μm), with a smaller back photocurrent in the region of porous silicon formation (region I). This is consistent with the intuitive idea that electrons photogenerated closer to the electrode surface are more sensitive to the influence of surface recombination centers and confirms the validity of experiments involving carrier photogeneration as a probe of the recombination phenomena involving injected electrons.

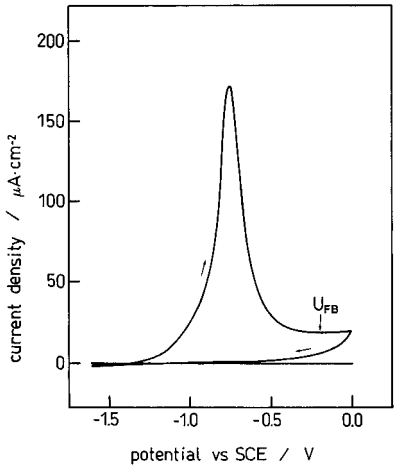

Figure 6. Cyclic voltammogram recorded in 2 M KOH at room temperature (scan rate 5 mV s^{-1}). The presumable position of the flatband potential (taken from ref 20) is indicated.

3.2. p-Si Dissolution in 2 M KOH. The open circuit potential of p-type (100) Si in 2.0 M KOH at room temperature is about −1.30 V (vs SCE). Although establishing the flatband potential for p-Si in this medium may not be trivial due to interference by oxide formation,[20−23,30] we adopt the value $U_{FB} \cong -0.2$ V vs SCE,[20] which is consistent with values for n-Si.[20,22,31]

Figure 6 shows the voltammogram obtained on cycling the potential of the fresh electrode between the limits of −1.6 V, at which hydrogen is slowly produced, and 0.0 V. Positive to open circuit, the current turns anodic and increases rapidly, showing a pronounced peak at about −0.75 V (vs SCE), after which it decreases again to a small plateau value. The dissolution peak at potentials largely negative to flatband is not consistent with a mechanism based on capture of holes from the valence band: a mechanism based on electron injection seems more likely.[23] On inverting the potential sweep at 0.0 V, a low current is recorded until the negative limit indicating passivation which has been attributed to formation of a compact oxide layer.[22,23]

3.2.1. Transistor-like Experiments in the Dark. In these experiments the back compartment was filled with the solution of 1 M NH_4F and the interface was polarized again as reported in section 3.1.1 ($U = -2.0$ V vs Pt). The potential of the front interface in contact with the alkaline solution was scanned from a value slightly negative of open circuit to a value considerably beyond the passivation peak (Figure 7, curve a).

The current detected by the indicator circuit (Figure 7, curve b) shows a low limiting value over most of the explored potential range, and a current peak at the onset of the dissolution peak. The back additional current drops to zero when the dissolution process has attained a typical integrated charge of 4−5 mC cm^{-2}, corresponding to oxidation of several monolayers. At this point, the dissolution current has not yet reached its maximum and the electrode potential is still considerably more negative than the assumed flatband value (compare Figure 6). Whether or not the fall in back current indicates a stop in injection processes associated with some change in dissolution mechanism may be clarified by experiments using light as a probe.

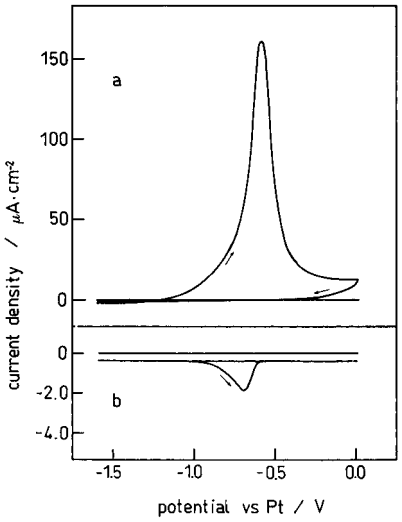

Figure 7. Experiment in a transistor-like arrangement. (upper curve a) Cyclic voltammogram recorded in 2 M KOH at the front interface in the dark (scan rate 5 mV s^{-1}). (lower curve b) Current in the indicator circuit.

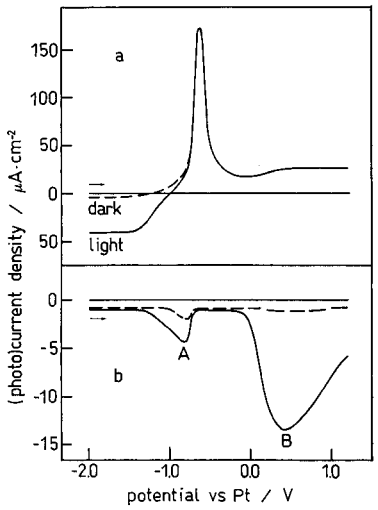

Figure 8. Experiment in a transistor-like arrangement. Dynamic current−potential curves (scan rate 5 mV s^{-1}, only positive-going scan from negative limit is reported) recorded in the dark (dashed lines) and under illumination (solid lines). (upper curve a) Current-potential curve in 2 M KOH, first potential sweep at a fresh electrode; (lower curve b) current in the indicator circuit.

3.2.2. Transistor-like Experiments under Illumination. In the first voltammogram recorded at a fresh electrode (Figure 8a) we observe in the negative potential range a limiting photocurrent corresponding to proton reduction with unit quantum efficiency Q. As the potential is swept in a positive direction, the front photocurrent starts decreasing due to less efficient collection and the onset of recombination phenomena, whereas the back photocurrent increases, passes through a maximum (Figure 8b, peak A), and then suddenly drops in a way very similar to the curve resulting from injection processes in the dark. On sweeping the potential further positive, the interface moves toward flatband and the front photoeffect disappears. The back photoeffect remains very small up to a potential in the passive region of the current−potential curve, which roughly corresponds to flatband potential U_{FB} (compare Figure 6), then it rapidly increases, attaining a maximum corresponding to back collection of about 30% of the photogenerated carriers (Figure 8b, peak B). This value is markedly larger than the value around 20% obtained in the experiments of Figure 5 and sets a lower limit for the "true" ratio $R = j_b/j_f$ which would be observed in the absence of surface recombination phenomena.[27] During the backward scan from the positive limit (not shown) the back current drops to a small value which is maintained over the region of peak B, then peak A is observed. On reaching the negative limit, all the photogenerated carriers are collected at the front interface and a photocurrent of proton reduction with $Q \cong 1$ is recovered.

In the second cycle (not shown), the voltammogram recorded by the front circuit shows a flat anodic form due to electrode passivation by an oxide layer. Remarkably, the presence of the surface oxide does not significantly alter the photocurrent of proton reduction collected at the negative potential limit, as already observed for proton reduction in the dark at oxidized n-Si.[23] The back circuit does not record any significant injection current in the dark, whereas the photocurrent curve exhibits the same two peaks A and B of Figure 8b, with some changes in position and shape probably due to the thick oxide layer which alters the potential distributions.

4. Discussion and Conclusions

The presently accepted mechanism for (photo)electrodissolution of n-Si in acidic fluoride, in the region of porous silicon formation, is based on a first step of hole capture followed by electron injection and further reaction of divalent silicon with the solvent to produce hydrogen:[5]

Scheme 1

$$Si(0) + h^+ \rightarrow Si(I) \qquad \text{hole capture} \quad (1a)$$

$$Si(I) \rightarrow Si(II) + e^- \qquad \text{electron inj.} \quad (1b)$$

$$Si(II) + 2\,H^+ \rightarrow Si(IV) + H_2 \qquad H_2 \text{ evolution} \quad (1c)$$

Assuming that the same mechanism occurs at p-Si, our experiments show that electrons generated in the conduction band either by the electrode process 1b or by light undergo rapid recombination (Figure 5b, $U < U_1$). The latter is probably promoted by surface states which are located at bandgap positions swept by the Fermi level at the onset of electrode dissolution.[28] Hence, the lack of an additional current in the indicator circuit, previously taken as evidence that divalent Si dissolution occurs via capture of two holes from the valence band[19] is actually compatible with Scheme 1. However, due to the much larger hole concentration in p-Si under direct bias than in n-Si under moderate illumination, we cannot discard the hypothesis that the second oxidation step may occur at p-Si partially via hole capture.

In the curves of Figure 5c the ratio $R = j_{b,ph}/j_{f,ph}$ attains a first maximum (peak A, $R \cong 0.20$) around open circuit. Under these conditions surface recombination is low but not negligible, as proved by the fact that comparatively higher ratios are obtained during experiments in KOH (Figure 8, $R \cong 0.30$ at peak B). A second maximum of R is observed in Figure 5c at a potential intermediate between U_1 and U_2 (peak B), corresponding to electropolishing with growth of a "wet" oxide.[5,9,10] At this potential, surface recombination is low again, then it increases in the region of the second electropolishing plateau ("dry" oxide[9,10]). The ratio relevant to electron injection in the dark by the dissolving species (Figure 5c, filled triangles) attains a maximum (corresponding to collection of a current $j_b \cong 0.005\ j_f$) in about the same potential region of peak B, representing a minimum of recombination rate. This coincidence emphasizes a crucial point: the back current is the result of injection and recombination phenomena and access to the "true" injection rate is not provided by these experiments alone. The current in the

indicator circuit never drops to zero up to the positive potential limit, beyond U_3. Remarkably, even hydrogen evolution is observed over the entire electropolishing plateau.[5] Hence, reactions 1b and 1c are not limited to the region of porous silicon formation but extend into the electropolishing regime.

Results obtained in alkaline medium confirm the phenomena of electron injection during dissolution, particularly at the fresh surface, previously proposed on the basis of indirect evidence.[22] Maximum back current is observed in the dark at the onset of the passivation peak, in a potential range in which recombination is low as shown by a fairly large back photocurrent (Figure 8b, peak A). On the basis of the assumed flatband (Figure 6), in this potential region the electrode is still polarized under depletion. In the range from onset to peak, the back current is a fraction of the front current in the range 2.5%−4%, depending on experiments. If we assume that all the front current is sustained by an injection mechanism, the back collection is much smaller than would be expected on the basis of mere bulk recombination (compare, for example, the maximum ratio $R \cong 0.30$ reported in Figure 8); hence, most of the injected electrons must recombine in the surface region. As the electrode potential is swept further in a positive direction both the photo and dark components of the back current drop together. This resembles what happens in acidic fluoride in the region of porous silicon formation: the drop (or absence) of back collected current does not originate from a drop (or absence) of injection processes, but rather indicates that the potential of the front interface has entered a region of active surface recombination centers, keeping the population of minority carriers low despite injection phenomena. On continuing the sweep toward positive potentials beyond the dissolution peak, an oxide layer is grown: the electrode potential enters the accumulation region and the back collected photocurrent increases and attains a maximum (peak B in Figure 8b). This corresponds to a minimum in surface recombination rate for an oxide passivated surface, a condition resembling that of peak B in Figure 5c.

In conclusion, investigations performed in a transistor-like geometry provide direct evidence of electron injection processes occurring at Si electrodes during dissolution in both acidic fluoride and alkaline media. The technique has an intrinsic limitation in the fact that the back collected (photo)current results from the interplay of injection and recombination phenomena at the surface under study: access to the "true" injection rates is precluded. Experiments based on light generation of minority carriers show that recombination at the front surface is minimum in two potential regions: close to open circuit potential (peak A) and under anodic polarization with formation of a surface oxide (peak B). Large recombination phenomena observed in the intermediate potential range may correspond to a region of active surface recombination centers.

Although the data cannot provide an accurate quantitative picture, they offer additional information on both injection and recombination processes which appears qualitatively consistent with the established current models for silicon dissolution.[5,22,23]

Acknowledgment. This work was performed during a visit by S. Cattarin to Bath University, supported by a study visit award of the Royal Society, London, which is gratefully acknowledged.

References and Notes

(1) Ulhir, A. *Bell Syst. Tech. J.* **1956**, *35*, 333.
(2) Turner, D. R. *J. Electrochem. Soc.* **1958**, *105*, 402. Turner, D. R. *J. Electrochem. Soc.* **1960**, *107*, 810.
(3) Chazalviel, J.-N. *Electrochim. Acta* **1992**, *37*, 865.
(4) Chazalviel, J.-N.; Ozanam, F.; Etman, M.; Paolucci, F.; Peter, L. M.; Stumper, J. *J. Electroanal. Chem.* **1992**, *327*, 343.
(5) Blackwood, D. J.; Borazio, A.; Greef, R.; Peter, L. M.; Stumper, J. *Electrochim. Acta* **1992**, *37*, 889.
(6) Lewerenz, H.-J.; Aggour, M. *J. Electroanal. Chem.* **1993**, *351*, 159.
(7) Ozanam, F.; Chazalviel, J.-N.; Radi, A.; Etman, M. *Ber. Bunsenges. Phys. Chem.* **1991**, *95*, 98.
(8) Venkateswara Rao, A.; Ozanam, F.; Chazalviel, J.-N. *J. Electrochem. Soc.* **1991**, *138*, 153.
(9) Ozanam, F.; Chazalviel, J.-N. *J. Electron Spec. Rel. Phenomena* **1993**, *64/65*, 395.
(10) Chazalviel, J.-N. In *Porous Silicon Science and Technology*, Vial, J. C., Derrien, J., Ed., Springer Verlag: Berlin (and Les Editions de Physique Les Ulis) 1995; p 17.
(11) Smith, R. L.; Collins, S. D. *J. Appl. Phys.* **1992**, *71*, R1.
(12) Eddowes, M. J. *J. Electroanal. Chem.* **1990**, *280*, 297.
(13) Matsumura, M.; Morrison, S. R. *J. Electroanal. Chem.* **1983**, *147*, 157.
(14) Peter, L. M.; Borazio, A. M.; Lewerenz, H.-J.; Stumper, J. *J. Electroanal. Chem.* **1990**, *290*, 229.
(15) Stumper, J.; Peter, L. M. *J. Electroanal. Chem.* **1991**, *309*, 325.
(16) Brattain, W. H.; Garrett, C. G. B. *Bell System Technol. J.* **1955**, *34*, 129.
(17) Myamlin, V. A.; Pleskov, Yu.V. In *Electrochemistry of Semiconductors*; Plenum Press: New York, 1967; p 213.
(18) Gerischer, H. In *Physical Chemistry*; Eyring, H.; Henderson, D., Jost, W., Eds.; Academic Press, New York, 1970; Vol. IXA, Chapter 5.
(19) Memming, R.; Schwandt, G. *Surf. Sci.* **1966**, *4*, 109. Memming, R.; Schwandt, G. *Surf. Sci.* **1966**, *5*, 97.
(20) Glembocki, O. J.; Stahlbush, R. E.; Tomkiewicz, M. *J. Electrochem. Soc.* **1985**, *132*, 145.
(21) Smith, R. L.; Kloeck, B.; De Rooij, N.; Collins, S. D. *J. Electroanal. Chem.* **1987**, *238*, 103.
(22) Allongue, P.; Costa-Kieling, V.; Gerischer, H. *J. Electrochem. Soc.* **1993**, *140*, 1009. Allongue, P.; Costa-Kieling, V.; Gerischer, H. *J. Electrochem. Soc.* **1993**, *140*, 1018.
(23) Bressers, P. M. M. C.; Pagano, S. A. S. P.; Kelly, J. J. *J. Electroanal. Chem.* **1995**, *391*, 159.
(24) Cattarin, S.; Musiani, M. *J. Electrochem. Soc.* **1995**, *142*, 3786.
(25) Cattarin, S.; Dietz, N.; Lewerenz, H.-J. *J. Electrochem. Soc.* **1994**, *141*, 1095.
(26) Paolucci, F.; Peter, L. M.; Stumper, J. *J. Electroanal. Chem.* **1992**, *341*, 165.
(27) Cattarin, S.; Peter, L. M., submitted to *J. Phys. Chem.*
(28) Searson, P. C.; Zhang, X. G. *Electrochim. Acta* **1991**, *36*, 499.
(29) Cattarin, S.; Chazalviel, J.-N.; Da Fonseca, C.; Ozanam, F.; Peter, L. M.; Schlichthörl, G.; Stumper, J., in preparation.
(30) Abbott, A. P.; Schiffrin, D. J.; Campbell, S. A. *J. Electroanal. Chem.* **1992**, *328*, 355.
(31) Chen, L.-C.; Chen, M.; Lien, C.; Wan, C.-C. *J. Electrochem. Soc.* **1995**, *142*, 170.